



Wynne, K. (2017) The mayonnaise effect. *Journal of Physical Chemistry Letters*, 8(24), pp. 6189-6192. (doi:[10.1021/acs.jpcllett.7b03207](https://doi.org/10.1021/acs.jpcllett.7b03207))

This is the author's final accepted version.

There may be differences between this version and the published version. You are advised to consult the publisher's version if you wish to cite from it.

<http://eprints.gla.ac.uk/153368/>

Deposited on: 14 December 2017

Enlighten – Research publications by members of the University of Glasgow

<http://eprints.gla.ac.uk>

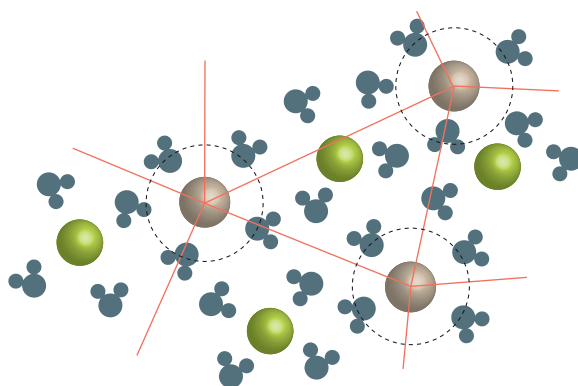
# The Mayonnaise Effect

Klaas Wynne

School of Chemistry, University of Glasgow, UK

**Abstract:** Structuring caused by the mixing of liquids or the addition of solutes to a solvent causes the viscosity to increase. The classical example is mayonnaise: a mixture of two low viscosity liquids, water and oil, is structured through the addition of a surfactant creating a dispersed phase, causing the viscosity to increase a thousandfold. The dramatic increase in viscosity in highly concentrated solutions is a long-standing unsolved problem in physical chemistry. Here we will show that this viscosity increase can be understood in terms of the solute-induced structuring of the first solvation shell leading to a jamming transition at a critical concentration. As the jamming transition is approached, the viscosity naturally increases according to a Vogel-Fulcher-Tammann type expression. This result calls into question the validity of the Jones-Dole B-coefficient as an indicator of structure making or breaking ability of solutes.

## TOC



**Keywords:** solutions, viscosity, jamming, Debye-Hückel, Jones-Dole, solvation, ionic liquids, deep eutectic solvents

It is well known that adding solutes to a solvent will alter the viscosity. In salt solutions at relatively low concentrations, the change in viscosity can be understood in terms of the drag exerted by the ion atmosphere that surrounds the ion, causing it to slow down, leading to an increase in the viscosity. This is described by the Debye-Hückel theory and has a square root dependence on the concentration. At higher concentrations, the viscosity can either increase or decrease. This is typically described by the empirical Jones-Dole expression<sup>1</sup>

$$\eta / \eta_0 = 1 + A\sqrt{x} + Bx, \quad (1)$$

where  $\eta/\eta_0$  is the normalized concentration-dependent viscosity,  $x$  the solute concentration,  $A$  is a coefficient that can be calculated from Debye-Hückel theory, and  $B$  an empirical coefficient.<sup>2-3</sup> The Jones-Dole  $B$  coefficient is often used to classify ions as either structure makers (kosmotropes) or structure breakers (chaotropes) according to their supposed strengthening or weakening of the hydrogen-bond network of water.<sup>4-6</sup>

The Jones-Dole expression works well up to about 1 M. At higher concentrations, it spectacularly breaks down as the viscosity of all solutions increase rapidly at high concentrations. The anomalous high concentration dependence of viscosity with solute concentration has not been addressed by a microscopic theory.

In a 1906 paper, Einstein already observed that a solute molecule might be considered large compared to the solvent molecules and therefore behave much like a suspended particle.<sup>7</sup> In dilute solution, he derived an expression for the change in viscosity

$$\eta / \eta_0 = 1 + 4\phi, \quad (2)$$

where  $\phi$  is the volume fraction of the suspended “particles”. The factor of 4 comes about because it was assumed that a solute molecule grabs hold of a solvation shell of water molecules with about three times the volume of the solute. In later work, quadratic, cubic, and higher order terms as well as exponential dependencies on  $\phi$  were added to take into account interactions between suspended particles.<sup>8-9</sup>

Here we will take a different approach. In the theory of supercooled liquids and glasses, the shear viscosity increases with decreasing temperature.<sup>10-11</sup> As the glass transition is approached, viscosity diverges away from simple Arrhenius behavior but may be described using the Vogel-Fulcher-Tammann (VFT) equation

$$\eta \propto \exp\left(\frac{D}{T-T_0}\right), \quad (3)$$

where  $T_0$  is the critical temperature corresponding to the glass transition and  $D$  is the fragility parameter.<sup>12</sup> The interpretation of the VFT equation is that as the temperature is lowered, the barrier for rearranging the liquid structure increases (due to the increasing extent of cluster formation) resulting in super-Arrhenius behavior of the temperature-dependent viscosity. At the critical temperature, the barrier becomes infinite and the system ‘jams’ to form a solid-like state.

The concept of jamming also occurs in soft condensed-matter physics. For example, a suspension of colloidal particles can jam when a critical concentration of particles is reached. This may be expressed by a similar expression as

$$\eta \propto \exp\left(\frac{D}{\phi_0 - \phi}\right), \quad (4)$$

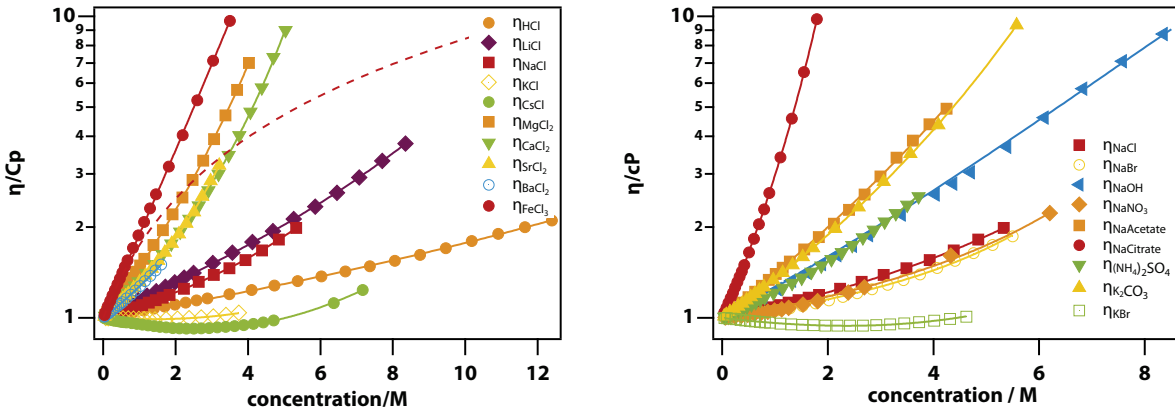


**Figure 1.** The macroscopic shear viscosity of aqueous salt solutions at 20°C. (left) Alkali and alkaline earth chlorides. (right) Various salts. Notice that the viscosity scale is logarithmic. The dashed line in the left-hand side panel is the linear (Jones-Dole B) approximation of the viscosity of FeCl<sub>3</sub>. The solid lines are fits to the data using the Vogel-Fulcher-Tamman-like expression shown in Eq. (6) with  $A = B = 0$  except for LiCl ( $A \neq 0$ ) and KCl, KBr, and CsCl ( $B \neq 0$ ).

where  $\phi$  is the packing fraction and  $\phi_0$  the critical packing fraction.<sup>13</sup> The concepts of glass formation and jamming are now generally considered to be equivalent within a model that considers temperature, packing density, and shear force.<sup>14-16</sup>

Ions in aqueous solution hold on more or less tightly to a solvation shell consisting of on the order of 4 to 8 water molecules. The key parameter to consider is the residence time of a water molecule in the solvation shell. While the residence time in the first shell around water itself is about 4 ps<sup>17</sup> and has similar values for ions such as chloride, ions with a high surface charge density because of their small size (e.g., Li<sup>+</sup>) or large charge (e.g., Fe<sup>3+</sup>) have residence times as large as hundreds of picoseconds. Thus, such ions effectively structure the surrounding liquid by forming clusters that can be regarded as soft spheres. Therefore, as the concentration of the salt increases, one expects a VFT-like dependence of viscosity on concentration, that is,

$$\eta \propto \exp\left(\frac{D}{x_0 - x}\right), \quad (5)$$

where  $x_0$  is the jamming concentration.

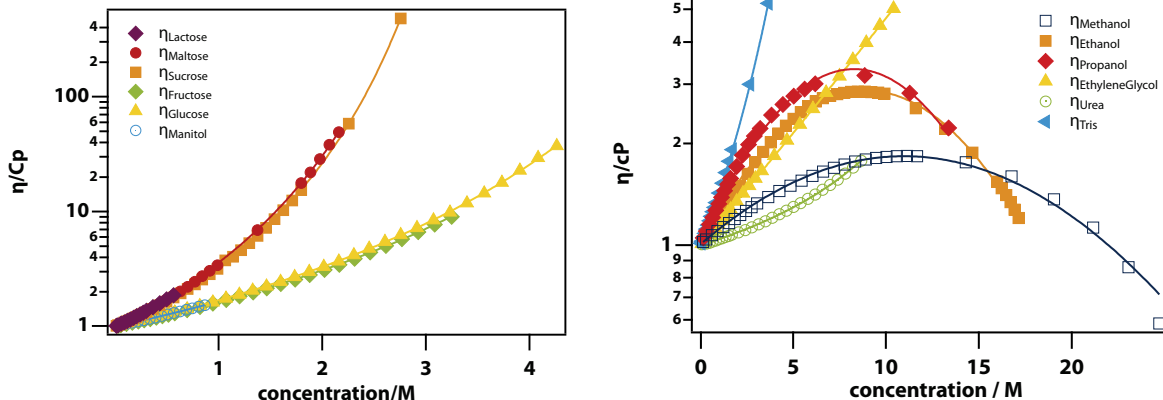


**Figure 2.** The macroscopic shear viscosity of solutions of neutral solutes at 20°C. Data on sugars (left) and other neutral solute molecules (right). The solid lines are fits to the data using Eq. (6) while the data for the simple alcohols use the modification in Eq. (8). The highest concentration shown for methanol, ethanol, and propanol corresponds to the pure alcohol.

This idea was tested by using published concentration dependent viscosity data.<sup>18</sup> These data are fitted using the expression

$$\eta/\eta_0 = A\sqrt{x} + Bx + \exp\left(\frac{D}{x_0 - x}\right)\exp\left(-\frac{D}{x_0}\right), \quad (6)$$

which goes to 1 for  $x = 0$  and where  $A = 0$  except for LiCl and  $B = 0$  except for three cases involving structure breaking ions. The critical concentration is calculated from the critical radius  $r_0$  using

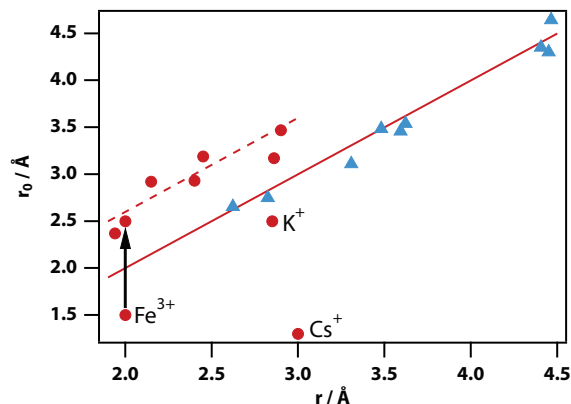
$$x_0 = \frac{3}{4\pi r_0^3 N_A 10^3}. \quad (7)$$

Figure 1 shows the concentration dependent viscosities of a range of salts in aqueous solution. In all cases there is a dramatic deviation from the linear Jones-Dole dependence. All of the data sets can be fit using Eq. (6) with  $B = 0$ , except in the case of KCl, KBr, and CsCl, which are well known structure breakers. In most cases, adding the Debye-Hückel  $A$  term does not improve the fit. The exception is the LiCl solutions in which the sum of squared residuals is reduced by 10 $\times$  by including the  $A$  term. Figure 2 shows the same for a number of sugars and a selection of other neutral solutes. The model works reasonably well even for some liquid mixtures such as  $n$ -alcohols and ethylene glycol but starts to break down for the former at high concentration. A reasonable fit can still be obtained when the jamming term is replaced by

$$\exp\left(\frac{D}{x_0 - x + Fx^2}\right), \quad (8)$$

which is a purely empirical modification.

The fit parameters for the fits shown in Figure 1 and Figure 2 are listed in Table S1 and Table S2, and plotted in Figure 3 as a function of the expected radius, that is, either the ion-water oxygen distance for the cations or the radius calculated from the density of the pure substance for the neutral molecules. As can be seen in Figure 3, most cations fall on a line that is  $\sim 0.6$  Å higher than the expected radius. This is the extra radial distance from the oxygen to the hydrogen in the ion-water complex. The neutral molecules all produce critical radii equal to the predicted radius consistent with a solvation shell playing no apparent role in jamming. Clear exceptions are  $K^+$  and  $Cs^+$ , which have a much lower critical radius (that is, a much higher critical concentration) than expected. Both ions are well known structure breakers and require  $B < 0$  in order to fit the viscosity data. Another exception is  $Fe^{3+}$ , where the fit with Eq. (6) gives an anomalously small critical radius. However, fitting the data with Eq. (8) instead gives a much improved fit and a much more reasonable critical radius. The data for the liquid mixtures of water with ethanol and ethylene glycol can also be fit well with Eq. (8) but the value of the critical radius is lower than expected.



**Figure 3. The critical radii of ions and neutral solutes.** Critical radii of a selection of ions (red disks) and neutral solutes (blue triangles) obtained by fitting the viscosity vs. concentration data using Eq. (6) against the radius predicted using the ion–water oxygen distance (for the ions) or the radius predicted from the density of the pure substance (neutral molecules). The data point labeled  $Fe^{3+}$  was obtained by a fit to Eq. (6), while the arrow points to the value obtained by fitting to Eq. (8).

Thus, it is now evident that the large increase in viscosity as a function of solute concentration seen in all solutions above about 1 M is the simple effect of a jamming transition at a high concentration. The range of radii shown in Figure 3 (2–4.5 Å) corresponds to critical concentrations from  $\sim 5$  to 50 M. In most cases, these concentrations are above the saturation concentration. For example, the critical concentration of LiCl is 30 M, which is well above the room temperature saturation concentration of about 10 M. However, the jamming transition at a fictive concentration causes an increase in the viscosity at low concentrations. The increase in viscosity caused by a jamming transition only weakly depends on the chemical properties of the solute and solvent molecules, and can therefore be thought of as essentially a colligative property.

Here only the effect of the cation on the viscosity was considered. Chloride was chosen as the common counterion as it is known that it has relatively little effect on the solvent structure and dynamics.<sup>2</sup> In particular, the residence time of a water molecule in the first solvation shell of chloride and water is about the same at 3 ps.<sup>17</sup> However, as can be seen in Table S1, the critical radius for NaBr ( $3.29 \pm 0.02$ ) is significantly greater than that of NaCl ( $2.93 \pm 0.02$ ) showing the effect of the larger anion on the location of the jamming transition. Note that the residence time of water in the first solvation shell of sugars is also relatively short ( $\sim 10$  ps)<sup>19</sup> explaining why the critical radius equals the predicted radius without including an additional water shell.

The jamming transition requires a system of “particles” in which translational motion is frozen at a critical concentration. Therefore, it is notable that the model works at all for liquid mixtures (*i.e.*, methanol, ethanol, propanol, and ethylene glycol in water). However, in this case true jamming cannot be achieved as the

solute is itself a liquid that can flow and hence the viscosity decreases again as the concentration approaches that of the pure alcohol. The empirically modified equation (Eq. (8)) partially takes this into account. Note that the viscosity of mayonnaise (also a mixture of two liquids) is extremely high because the use of a surfactant gives rise to droplets with a radius on the order of micrometers rather than Ångströms. An intermediate case occurs in (room-temperature) ionic liquids where mesoscopic scale clustering gives rise to anomalously high liquid viscosities due to the jamming effect.<sup>20–22</sup> The mayonnaise effect is also likely to be at play in highly viscous deep eutectic solvents<sup>23</sup> as well as the critical increase in viscosity in liquid mixtures near the liquid-liquid critical point.<sup>24</sup>

Similar expressions to Eq. (5) have been used previously. For example, solution conductivity and viscosity have been described by a Vogel-Fulcher-Tammann like expression<sup>25</sup> although without reference to the concept of jamming. The concept of jamming has been invoked previously in describing the viscosity of protein solutions,<sup>26–27</sup> which are of course more intuitively similar to colloidal suspensions. The idea of a relatively rigid solvation shell around ions giving rise to an increased viscosity through the Einstein expression Eq. (2) has been invoked previously.<sup>28</sup>

The jamming effect does not require an anomalous enhancement of the structure of the solvent around the solute<sup>29</sup> nor does it require cooperative effects.<sup>30</sup> It is an effect that will always occur and is therefore critically important in assessing whether particular solutes are structure makers or breakers.<sup>31–32</sup> Note that a structure-making effect ( $B > 0$ ) is not required to fit any of the data, however, for three solutes (KCl, KBr, and CsCl) a structure-breaking effect ( $B < 0$ ) is required. This implies that concentration-dependent viscosities of solutions cannot provide evidence of structure-

making ability (kosmotropicity) requiring a reevaluation of this concept.<sup>6</sup> Concentration-dependent viscosities have been widely fit to the Jones-Dole equation failing dramatically above 1 M. It is now clear that jamming, an effect that may be referred to as the “mayonnaise effect”, is responsible for this failure.

## SUPPORTING INFORMATION

The Supporting Information is available free of charge on the ACS Publications website: Fit parameters (PDF).

## AUTHOR INFORMATION

### Corresponding Author

\*klaas.wynne@glasgow.ac.uk

### Notes

The author declares no competing financial interest.

## ACKNOWLEDGMENT

I thank the Engineering and Physical Sciences Research Council (EPSRC) for support through grants EP/E046541/2, EP/F06926X/2, EP/J009733/1, and EP/K034995/1.

## REFERENCES

1. Jones, G.; Dole, M. The Viscosity of Aqueous Solutions of Strong Electrolytes with Special Reference to Barium Chloride. *J. Am. Chem. Soc.* **1929**, *51* (10), 2950-2964.
2. Jenkins, H.; Marcus, Y. Viscosity B-Coefficients of Ions in Solution. *Chem. Rev.* **1995**, *95* (8), 2695-2724.
3. Jiang, J.; Sandler, S. A New Model for the Viscosity of Electrolyte Solutions. *Industrial & Eng. Chem. Res.* **2003**, *42* (25), 6267-6272.
4. Mancinelli, R.; Botti, A.; Bruni, F.; Ricci, M. A.; Soper, A. K. Perturbation of Water Structure Due to Monovalent Ions in Solution. *Phys. Chem. Chem. Phys.* **2007**, *9* (23), 2959-2967.
5. Marcus, Y. Effect of Ions on the Structure of Water: Structure Making and Breaking. *Chem. Rev.* **2009**, *109* (3), 1346-1370.
6. Ball, P.; Hallsworth, J. E. Water Structure and Chaotropy: Their Uses, Abuses and Biological Implications. *Phys. Chem. Chem. Phys.* **2015**, *17* (13), 8297-8305.
7. Einstein, A. Eine Neue Bestimmung Der Moleküldimensionen. *Ann. Physik* **1906**, *324* (2), 289-306.
8. Thomas, D. G. Transport Characteristics of Suspension: VIII. A Note on the Viscosity of Newtonian Suspensions of Uniform Spherical Particles. *J. Colloid Sci.* **1965**, *20* (3), 267-277.
9. Laliberté, M. Model for Calculating the Viscosity of Aqueous Solutions. *J. Chem. Eng. Data* **2007**, *52* (2), 321-335.
10. Angell, C. A.; Ngai, K.; McKenna, G.; Mcmillan, P.; Martin, S. Relaxation in Glassforming Liquids and Amorphous Solids. *J. Appl. Phys.* **2000**, *88* (6), 3113-3157.
11. Debenedetti, P.; Stillinger, F. Supercooled Liquids and the Glass Transition. *Nature* **2001**, *410* (6825), 259-267.
12. Angell, C. A. Liquid Fragility and the Glass Transition in Water and Aqueous Solutions. *Chem. Rev.* **2002**, *102* (8), 2627-2649.
13. Watanabe, K.; Tanaka, H. Direct Observation of Medium-Range Crystalline Order in Granular Liquids near the Glass Transition. *Phys. Rev. Lett.* **2008**, *100* (15), 158002.
14. Liu, A.; Nagel, S. Nonlinear Dynamics - Jamming Is Not Just Cool Any More. *Nature* **1998**, *396* (6706), 21-22.
15. Zhang, Z.; Xu, N.; Chen, D. T. N.; Yunker, P.; Alsayed, A. M.; Aptowicz, K. B.; Habdas, P.; Liu, A. J.; Nagel, S. R.; Yodh, A. G. Thermal Vestige of the Zero-Temperature Jamming Transition. *Nature* **2009**, *459* (7244), 230-233.
16. Mari, R.; Krzakala, F.; Kurchan, J. Jamming Versus Glass Transitions. *Phys. Rev. Lett.* **2009**, *103* (2), 025701.
17. Laage, D.; Hynes, J. Reorientational Dynamics of Water Molecules in Anionic Hydration Shells. *Proc. Natl. Acad. Sci. USA* **2007**, *104* (27), 11167-11172.
18. *Handbook of Chemistry and Physics*. CRC Taylor and Francis: 2006; Vol. 87.
19. Winther, L. R.; Qvist, J.; Halle, B. Hydration and Mobility of Trehalose in Aqueous Solution. *J. Phys. Chem. B* **2012**, *116* (30), 9196-9207.
20. Cosby, T.; Vicars, Z.; Wang, Y.; Sangoro, J. Dynamic-Mechanical and Dielectric Evidence of Long-Lived Mesoscale Organization in Ionic Liquids. *J. Phys. Chem. Lett.* **2017**, *8* (15), 3544-3548.
21. Russina, O.; lo Celso, F.; Plechkova, N. V.; Triolo, A. Emerging Evidences of Mesoscopic-Scale Complexity in Neat Ionic Liquids and Their Mixtures. *J. Phys. Chem. Lett.* **2017**, *8* (6), 1197-1204.
22. Turton, D. A.; Hunger, J.; Stoppa, A.; Hefter, G.; Thoman, A.; Walther, M.; Buchner, R.; Wynne, K. Dynamics of Imidazolium Ionic Liquids from a Combined Dielectric Relaxation and Optical Kerr Effect Study: Evidence for Mesoscopic Aggregation. *J. Am. Chem. Soc.* **2009**, *131* (31), 11140-11146.
23. Smith, E. L.; Abbott, A. P.; Ryder, K. S. Deep Eutectic Solvents (Dess) and Their Applications. *Chem. Rev.* **2014**, *114* (21), 11060-11082.
24. Debye, P.; Chu, B.; Woermann, D. Viscosity of Critical Mixtures. *J. Polym. Sci. A* **1963**, *1*, 249-254.
25. Angell, C. A.; Bressel, R. Fluidity and Conductance in Aqueous-Electrolyte Solutions - Approach from Glassy State and High-Concentration Limit .1. Ca(NO<sub>3</sub>)<sub>2</sub> Solutions. *J. Phys. Chem.* **1972**, *76* (22), 3244-3253.
26. Ross, P. D.; Minton, A. P. Hard Quasispherical Model for the Viscosity of Hemoglobin Solutions. *Biochem. Biophys. Res. Commun.* **1977**, *76* (4), 971-976.
27. Gonçalves, A. D.; Alexander, C.; Roberts, C. J.; Spain, S. G.; Uddin, S.; Allen, S. The Effect of Protein Concentration on the Viscosity of a Recombinant Albumin Solution Formulation. *RSC Adv.* **2016**, *6* (18), 15143-15154.
28. Omta, A.; Kropman, M.; Woutersen, S.; Bakker, H. J. Negligible Effect of Ions on the Hydrogen-Bond Structure in Liquid Water. *Science* **2003**, *301* (5631), 347-349.
29. Frank, H. S.; Evans, M. W. Free Volume and Entropy in Condensed Systems Iii. Entropy in Binary Liquid Mixtures; Partial Molal Entropy in Dilute Solutions; Structure

- and Thermodynamics in Aqueous Electrolytes. *J. Chem. Phys.* **1945**, *13* (11), 507-532.
30. Tielrooij, K. J.; Garcia-Araez, N.; Bonn, M.; Bakker, H. J. Cooperativity in Ion Hydration. *Science* **2010**, *328* (5981), 1006-1009.
31. Hribar, B.; Southall, N. T.; Vlachy, V.; Dill, K. A. How Ions Affect the Structure of Water. *J. Am. Chem. Soc.* **2002**, *124* (41), 12302-12311.
32. Corridoni, T.; Mancinelli, R.; Ricci, M. A.; Bruni, F. Viscosity of Aqueous Solutions and Local Microscopic Structure. *J. Phys. Chem. B* **2011**, *115* (48), 14008-14013.
33. Koneshan, S.; Rasaiah, J.; Lynden-Bell, R.; Lee, S. Solvent Structure, Dynamics, and Ion Mobility in Aqueous Solutions at 25 Degrees C. *J. Phys. Chem. B* **1998**, *102* (21), 4193-4204.
34. Obst, S.; Bradaczek, H. Molecular Dynamics Study of the Structure and Dynamics of the Hydration Shell of Alkaline and Alkaline-Earth Metal Cations. *J. Phys. Chem.* **1996**, *100* (39), 15677-15687.
35. Spangberg, D.; Rey, R.; Hynes, J.; Hermansson, K. Rate and Mechanisms for Water Exchange around Li+(Aq) from Md Simulations. *J. Phys. Chem. B* **2003**, *107* (18), 4470-4477.
36. Guardia, E.; Laria, D.; Marti, J. Hydrogen Bond Structure and Dynamics in Aqueous Electrolytes at Ambient and Supercritical Conditions. *J. Phys. Chem. B* **2006**, *110* (12), 6332-6338.
37. Jiao, D.; King, C.; Grossfield, A.; Darden, T. A.; Ren, P. Simulation of Ca<sup>2+</sup> and Mg<sup>2+</sup> Solvation Using Polarizable Atomic Multipole Potential. *J. Phys. Chem. B* **2006**, *110* (37), 18553-18559.
38. Hofer, T. S.; Rode, B. M.; Randolph, B. R. Structure and Dynamics of Solvated Ba(II) in Dilute Aqueous Solution – an Ab Initio Qm/Mm Md Approach. *Chem. Phys.* **2005**, *312* (1-3), 81-88.
39. Remsungnen, T.; Rode, B. M. Qm/Mm Molecular Dynamics Simulation of the Structure of Hydrated Fe(II) and Fe(III) Ions. *J. Phys. Chem. A* **2003**, *107* (13), 2324-2328.

SUPPLEMENTARY INFORMATION

**Table S1. Viscosity data and fit parameters for a series of mono- and divalent cation salts.** Fit parameters  $A$ ,  $B$ , and  $F$  from Eq. (6) and (8), effective jamming radius  $r_0$ , the cation–water oxygen distance as obtained from MD simulations  $r_{ion-O}$  (Å), and the first shell residence time  $\tau_{MD}$ . The values of  $r_{ion-O}$  for potassium carbonate, sodium acetate, and sodium citrate haven been calculated from the density of the pure substances.

	$A$	$B$	$D$	$F$	$r_0/\text{Å}$	$r_{ion-O}$ (Å)	$\tau_{MD}$ (ps)
HCl	-	-	160 ± 14	-	1.89 ± 0.02	-	-
LiCl	0.032 ± 0.003	-	100 ± 6	-	2.37 ± 0.02	2.0 <sup>5, 33-35</sup>	41-101 <sup>33-36</sup>
NaCl	-	-	21.5 ± 0.8	-	2.93 ± 0.02	2.4-2.5 <sup>5, 33-34, 37</sup>	14.7-25 <sup>33-34, 36</sup>
KCl	-	-0.08 ± 0.04	41 ± 120	-	2.5 ± 0.9	2.8-2.9 <sup>5, 33-34, 37</sup>	8.2 <sup>33-34, 36</sup>
KBr	-	-0.16 ± 0.01	800 ± 1200	-	1.7 ± 0.4	<i>idem</i>	
CsCl	-	-0.18 ± 0.01	4100 ± 7400	-	1.3 ± 0.4	3.0 <sup>5, 36</sup>	6.9 <sup>36</sup>
MgCl <sub>2</sub>	-	-	92 ± 3	-	2.92 ± 0.01	2.1-2.2 <sup>5, 34, 37</sup>	422 <sup>34</sup>
CaCl <sub>2</sub>	-	-	39 ± 1.3	-	3.19 ± 0.01	2.4-2.5 <sup>5, 33-34, 37</sup>	700 <sup>33</sup>
SrCl <sub>2</sub>	-	-	22 ± 1	-	3.47 ± 0.02	2.9 <sup>34</sup>	51 <sup>34</sup>
BaCl <sub>2</sub>	-	-	34 ± 6	-	3.17 ± 0.08	2.86 <sup>38</sup>	18.6 <sup>38</sup>
FeCl <sub>3</sub>	-	-	9000 ± 3900	-	1.5 ± 0.1	2.0 <sup>39</sup>	106 <sup>39</sup>
<i>idem</i>			400 ± 400	0.02 ± 0.01	2.5 ± 0.4	<i>idem</i>	<i>idem</i>
(NH <sub>4</sub> ) <sub>2</sub> SO <sub>4</sub>	-	-	39 ± 2	-	3.02 ± 0.02	-	-
NaBr	-	-	7.2 ± 0.4	-	3.29 ± 0.02	-	-
NaOH	-	-	82 ± 5	.0269 ± 0.0003	2.74 ± 0.02	-	-
NaNO <sub>3</sub>	-	-	12 ± 2	-	3.09 ± 0.05	-	-
K <sub>2</sub> CO <sub>3</sub>	-	-	104 ± 2	-	2.75 ± 0.01	2.83	-
NaAcetate	-	-	260 ± 53	-	2.41 ± 0.08	2.77	-
NaCitrate	-	-	39.9 ± 0.6	-	3.92 ± 0.01	3.92	-

**Table S2. Viscosity data and fit parameters for a series of sugars and other neutral molecules.**

	$A$	$B$	$D$	$F$	$r_0/\text{Å}$	$r_{molecule}/\text{Å}$
Lactose	-	-	15 ± 2	-	4.644 ± 0.084	4.464
Maltose	-	-	25.4 ± 0.8	-	4.302 ± 0.017	4.450

<b>Sucrose</b>	-	-	22.12 ± 0.06	-	4.353 ± 0.001	4.406
<b>Fructose</b>	-	-	38.9 ± 0.8	-	3.486 ± 0.009	3.480
<b>D-glucose</b>	-	-	43.5 ± 0.8	-	3.458 ± 0.008	3.593
<b>D-mannitol</b>	-	-	37 ± 10	-	3.53 ± 0.15	3.622
<b>Urea</b>	-	-	17.7 ± 0.4	-	2.655 ± 0.007	2.623
<b>Tris(hydroxymethyl) aminomethane</b>	-	-	57 ± 1	-	3.11 ± 0.01	3.307
<b>Ethylene glycol</b>	-	-	25000 ± 4600	-	1.00 ± 0.03	2.806
<b>Methanol</b>	-	-	46000 ± 5 10 <sup>5</sup>	0.0456 ± 0.0003	0.85 ± 1.5	2.522
<b>Ethanol</b>	-	-	28000 ± 1 10 <sup>5</sup>	0.0558 ± 0.0002	1.04 ± 0.75	2.850
<b>Propanol</b>	-	-	62000 ± 6 10 <sup>5</sup>	0.0604 ± 0.0005	0.95 ± 1.5	3.096

**Table S3.** Molecular radii calculated from the density of the pure substance.

	<b>Molar mass (g/mol)</b>	<b>Density (g/cm<sup>3</sup>)</b>	<b>Radius (Å)</b>
<b>Lactose</b>	342.30	1.525	4.46443
<b>Maltose</b>	342.30	1.54	4.44989
<b>Sucrose</b>	342.30	1.587	4.40552
<b>Fructose</b>	180.16	1.694	3.48045
<b>D-glucose</b>	180.1559	1.54	3.59277
<b>D-mannitol</b>	182.172	1.52	3.62187
<b>Urea</b>	60.06	1.32	2.62255
<b>Tris</b>	121.14	1.328	3.30687
<b>K<sub>2</sub>CO<sub>3</sub></b>	138.205	2.43	2.82505
<b>NaAcetate</b>	82.03	1.528	2.77121
<b>Na<sub>3</sub>Citrate</b>	258.06	1.7	3.91872
<b>Ethylene glycol</b>	62.07	1.1132	2.80644
<b>Methanol</b>	32.04	0.792	2.52179
<b>Ethanol</b>	46.07	0.7893	2.84957
<b>n-Propanol</b>	60.10	0.803	3.0958